

Overview of the Lost Meteorites of Antarctica field campaigns

K. H. JOY ^{1*}, A. R. D. SMEDLEY¹, J. L. MACARTHUR ¹, W. van VERRE², L. A. MARSH²,
M. ROSE³, T. A. HARVEY¹, R. TARTÈSE ¹, R. H. JONES ¹, I. D. ABRAHAM⁴,
J. W. WILSON², A. J. PEYTON², L. GERRISH³, J. BAUM³, G. RAYMOND³, R. TAYLOR³, and
G. W. EVATT⁵

¹Department of Earth and Environmental Sciences, University of Manchester, Manchester, UK

²Department of Electrical and Electronic Engineering, University of Manchester, Manchester, UK

³British Antarctic Survey, Cambridge, UK

⁴Department of Applied Mathematics and Theoretical Physics, University of Cambridge, Cambridge, UK

⁵Department of Mathematics, University of Manchester, Manchester, UK

*Correspondence

K. H. Joy, Department of Earth and Environmental Sciences, University of Manchester, Manchester, UK.

Email: katherine.joy@manchester.ac.uk

(Received 21 August 2023; revision accepted 20 November 2023)

Abstract—The Lost Meteorites of Antarctica project was the first UK-led Antarctic meteorite recovery expedition. The project has successfully confirmed two new high-density meteorite stranding zones in the Hutichison Icefield and Outer Recovery Icefields areas and investigated the geology of three previously unvisited Antarctic nunataks (Turner Nunatak, Pillinger Nunatak, Halliday Nunatak). The project undertook meteorite searching on the ice surface via skidoo reconnaissance and systematic searching and developed a novel pulse induction metal detection system to search for englacial iron-rich meteorites trapped within the upper one meter of ice. In total, 121 meteorites have been recovered from the ice surface searching activities, which are now curated in the United Kingdom at the Natural History Museum London and are available for scientific analysis.

INTRODUCTION

Antarctica is the world's most prolific source of meteorite finds (Corrigan, 2011) with (as of June 2023) 43,864 classified stones, representing 61.1% (out of 71,778) of all classified meteorites with approved names in the *Meteoritical Bulletin*. This scientific reserve includes samples from the Moon, Mars, and asteroid parent bodies, helping scientists to investigate the origins and evolution of planetary bodies formed in different regions of our solar system (Wadhwa et al., 2020 and references therein).

The first meteorite collected in Antarctica was named Adelie Land, and is an L5 chondrite sample recovered by

the Australasian Antarctic Expedition of 1911–1914. Scientific expeditions by the United States and Japan in the 1970s (Kojima, 2006; Marvin, 2014 and references therein) formalized international scientific reconnaissance and systematic search programs which have now been operating for over 40 years (Corrigan, 2011 and references therein). Meteorite recovery campaigns to Antarctica's meteorite stranding zones (MSZs) have been regularly undertaken by teams from the United States, Japan, Belgium, Italy, European collaborations, China, and South Korea across Antarctica (Cassidy et al., 1992; Choi et al., 2009; Debaille et al., 2011; Delisle et al., 1993; Folco et al., 2002; Harvey et al., 2014; Imae et al., 2013; Park et al., 2015; Righter et al., 2014; Yoshida et al., 1971; Zhang & Haward, 2022; Zhou et al., 2011). Readers are referred to Cassidy (2012) and Harvey (2003), which provide thorough summaries of the history and rationale for Antarctic meteorite recovery efforts. These search

^aPreviously at Department of Electrical and Electronic Engineering, University of Manchester, Manchester, UK.

^bPreviously at British Antarctic Survey, Cambridge, UK.

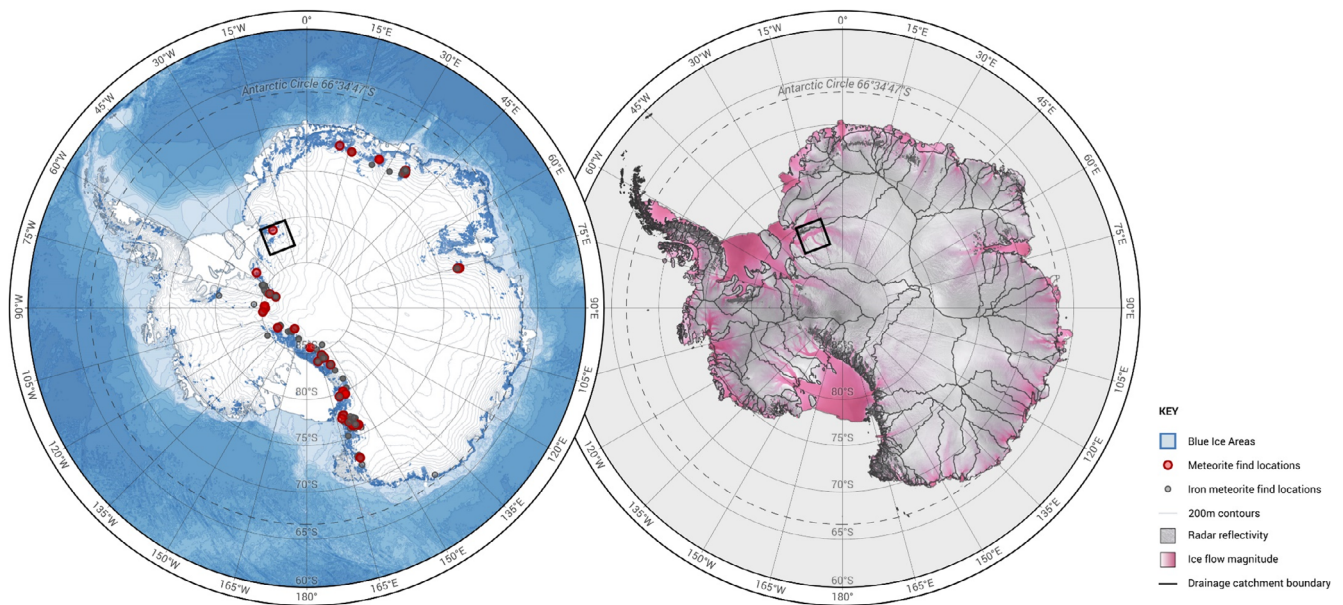


FIGURE 1. Regional view of Antarctica showing location of the field site highlighted in Figure 2 (black box). Left frame shows map of Antarctica with meteorite find locations (Met. Bull database) shown as red (all meteorites) and gray (iron-rich meteorites) symbols. Underlying elevation and bathymetry data taken from Bedmap2 (Fretwell et al., 2013). Right shows the surface ice flow relative velocity (Rignot et al., 2017) where increasing shades of pink colors (glaciers, ice shelves) denote faster ice flow speeds. Overlain are the basin catchment outlines obtained through the SCAR Antarctic Digital Database.

sites are often located adjacent to exposed and buried mountain ranges (Figure 1), where ice transported from the south polar plateau in ice sheets grounds on the underlying topography, forcing it to rise to the surface, where it slows and is eroded by strong katabatic winds, liberating the meteorites carried within (Annexstad, 1986; Cassidy, 2012; Corrigan, 2011; Corti et al., 2003; Faure, 1990; Harvey, 2003; Nagata, 1978; Whillans & Cassidy, 1983). These MSZ (surfaces) are often associated with blue ice (Bintanja, 1999), stranded ice tongues (Cassidy et al., 1987), and glacial moraines (Cassidy et al., 1992).

The Lost Meteorites of Antarctica Project was the first Antarctic meteorite recovery program to be led by the United Kingdom (<https://ukantarcticmeteorites.wordpress.com/>). The project was set up to search in blue ice regions of Antarctica for surface-located meteorites and subsurface meteorites trapped within the ice. The goals of the project were to test the hypothesis put forward by Evatt et al. (2016) that metallic iron-bearing meteorites (i.e., irons, stony irons, CB chondrites) with high degrees of thermal conductivity are preferentially heated by penetrating sunlight within ice, compared to iron-poor meteorites. This heating effect combined with their higher density is proposed to cause iron-rich meteorites to “sink” in comparison to the “upward” moving ice in which is it transported, meaning that iron-rich meteorites might never become exposed at the ice surface. Models by Smedley et al. (2020) suggest that

iron-rich meteorites might become “concentrated” in ice just below the surface at depths of ~10 cm, meaning they are not so readily available at the ice surface to be spotted and collected by meteorite recovery teams. Such a mechanism is proposed to explain the apparent statistical disparity between the populations of iron-rich and iron-poor meteorites found in Antarctica compared with rest of the world meteorite “finds” (i.e., samples found in deserts or other locations) and meteorite “falls” (i.e., samples recovered after observed fireball events) samples (e.g., Corrigan et al., 2014; Evatt et al., 2016). This paper provides background to the project’s two field campaigns, the field sites visited, and some initial summary findings.

FIELD CAMPAIGN PLANNING

The Lost Meteorites project undertook two Antarctic meteorite recovery expeditions in austral summers 2018–2019 and 2019–2020. The project was funded by the Leverhulme Trust, a charitable trust in the United Kingdom which supports interdisciplinary research. The British Antarctic Survey (BAS) agreed to support the field logistics part of the project including providing access to field sites, expert field guides, and expertise in polar equipment. Permission for the field campaigns was sought from BAS via an Award Operational Support Planning Questionnaire and, before the field activities, the project team completed relevant Preliminary

Environmental Assessments, along with health and safety risk assessments. As a requirement of the UK Government's Antarctic Act, collection of meteorites from the field sites was granted via the BAS Environment Office through a UK Foreign & Commonwealth Office Specialist Activity Permit. Field participants completed required polar fieldwork pre-deployment training. The Antarctic continent was reached via a flight from Punta Arenas, Chile, to the Rothera Research station on the West Antarctic peninsula (Figure 1). At Rothera, the field team participants received training in polar field skills, before deploying out to the field sites via Halley Research Station on BAS's Twin Otter aircrafts (see [Field Site Geological and Geomorphological Descriptions](#) Section). The two field campaigns visited the Outer Recovery (OUT) Icefields and Hutchison (HUT) Icefields in an area located south of the Shackleton Mountain Range (Figures 2–4). These sites were selected through an optimization process, using the latest geographic information of Antarctica's Blue Ice Areas (Hui et al., 2014). The first constraint was that any site had to be serviceable by BAS logistics (i.e., deep field aircraft access) from their Rothera and Halley research stations and deep field fuel depot sites. The next constraint was due to the design of the metal detector panels, which required the surface to be ice dominated, thereby ruling out areas of blue ice once mixed with moraine, where terrestrial rock may have compromised the panels. After this, heavily crevassed areas were removed from the list. This filtering left a number of potential MSZs. Given the project was only able to deploy the metal detector panels at one site, it meant that the site with the highest likelihood of meteorites needed to be robustly identified. To achieve this a glaciological/mathematical approach was developed, and the (subsequently named) Outer Recovery Icefields blue ice area was identified as a feasible area containing the highest number of meteorites, followed by the Hutchinson Icefield. This study later gave broader implications to meteorite fall fluxes worldwide, and was published in Evatt et al. (2020). But given the probabilistic nature of finding meteorites at any given site, an initial reconnaissance mission was required prior to full deployment, so as to confirm whether or not the selected potential MSZs actually held surface meteorites in quantities anything like those predicted. Fortunately, the reconnaissance mission to Outer Recovery in 2018–2019 (see [Field Campaign](#) Section) proved successful in hosting the largest number of meteorites, consistent with predictions. This meant the fuller 2019–2020 field campaign would base itself there (see [Field Campaign](#) Section). It also means that any future Antarctic meteorite collection missions can use the same methodology with a justified degree of confidence.

FIELD SITE GEOLOGICAL AND GEOMORPHOLOGICAL DESCRIPTIONS

Hutchison Icefield Description

Hutchison Icefield, located at 81°30'30" S, 26° 10' 00" W, comprises of a collection of blue icefields and two nunataks (Table S1). The icefield name is included in the UK Antarctic Gazetteer (<https://apc.antarctica.ac.uk/>), and is named after meteoriticist Prof. Robert Hutchison (1938–2017).

The icefields are located to the east of Whichaway Nunataks, and south of the Shackleton Mountain area of Coats Land (British Antarctic Territory, UK administered; Figures 2 and 4). The icefields sit ~50 km to the west of the Ramp ice stream (Figure 2). Ice flows into the region from the southwest from the south part of the Recovery Ice Stream basin catchment (Willis et al., 2016), at velocities between ~1 and 10 m year⁻¹ from the south-west (Rignot et al., 2011). The ice in this area includes a mix of blue ice suncupped (rippled) surfaces (~1 to 10 cm), white ice “rippled” (~1 to 3 cm high) and smooth surfaces, heavily crevassed zones, and ice rises (Figure 5a–d). The topography of the icefields is relatively flat with slopes typically <5°. The northern and westerly blue icefields are influenced by the surface expression of Turner nunatak (Figures 4 and 6). The southerly and easterly section of the blue icefields are bound to the east by a series of steep ice pinnacles and ridges (presumably denoting a buried topographic high), with heavily crevassed icefields located above (to the east) of topographic change. The western icefields on lower topography areas typically are crevasse free, apart from at the most westerly edge where the ice becomes whiter and disappears under permanent snow cover. Several of the icefields have sporadic small 50 cm to 1 m ice “hummocks,” equivalent of wave-like features in an otherwise relatively flat, navigable, ice surface. The Hutchison Icefield are all surface debris free, apart from the most westerly north icefield, closest to the Turner nunatak, which has some wind-blown surface rock debris from the nunatak. East of Turner nunatak is a small (~50 m long) ridge of englacial and surface rocks and boulders up to ~1 m in diameter. Tephra bands run across several of the icefields (north #2, south #3 and #4).

Turner nunatak, named after cosmochemist Prof. Grenville Turner (1936-present), which is located in the north of the icefields, is 1.64 × 0.70 km in size (Figure 4). The nunatak consists of layered sedimentary rocks (Figure 6a) including (i) bedded sandstone units (BAS sample # Z18-5-8: Figure S1), which hosts fossilized wood (we identified one complete log at the site and several tree stumps and trunk holes; Figure 6e), (ii) finer

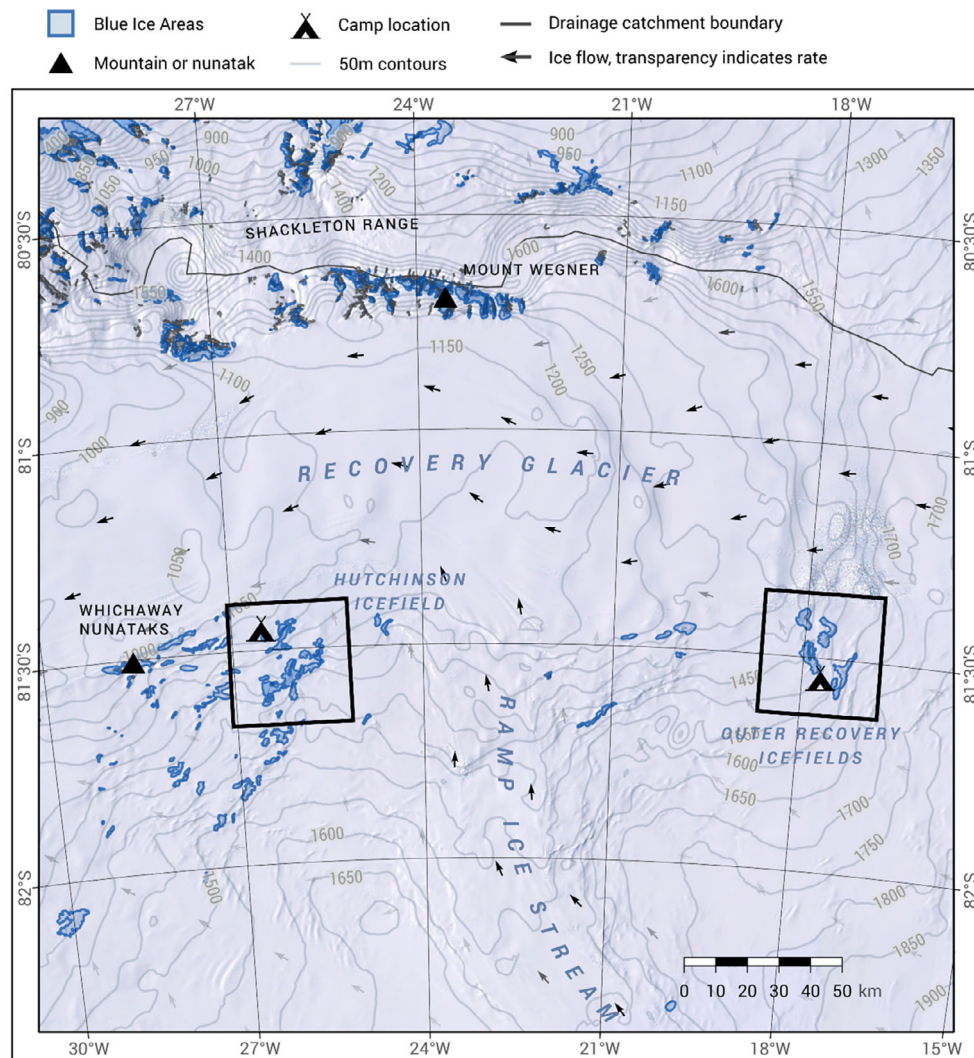


FIGURE 2. Recovery Glacier region, showing an area to the south of the Shackleton Mountain range. The two field areas—Hutchison Icefield to the west (Figure 4) and Outer Recovery Icefields to the east (Figure 3)—are denoted in black squares. Topography contours are derived from BEDMAP2 DEM (Fretwell et al., 2013). Blue ice areas are taken from Hui et al. (2014). Iceflow velocities from Rignot et al. (2017). Base map is Landsat Image Mosaic of Antarctica (LIMA).

silty units, and (iii) basaltic dykes and sills that are 0.5–1 m in diameter, cross-cutting the other lithologies (Figure 6a,c). A sample of one of the cross-cutting dykes (BAS sample # Z18-5-9; Figures S2 and S3) is hypocrySTALLINE, rich in feldspar and pyroxene microcrystals ($\sim 20 \times 200 \mu\text{m}$ in size; Figures S2 and S3), with small vesicles with calcite-rich amygdale infilling. The top surface of the nunatak is at ~ 1078 m altitude and is a desert pavement of arranged siltstone layers (Figure 6d,f), with dropstone erratics consisting of coral-rich limestones, basement igneous rocks, and finer grained sandstones.

Pillinger nunatak, named after planetary scientist Prof. Colin Pillinger (1943–2014), is located to the south

of the icefields and is $\sim 0.28 \times 0.28$ km (Figures 4 and 7a). The nunatak is formed of cross bedded and bedded sandstones with a basaltic dyke (Figure 7). The surface of the nunatak resides at ~ 1285 m and is covered with mostly snow and periglacially sorted rocks (Figure 7d). Erratics observed on the top surface of the nunatak are only igneous and metamorphic basement rocks; no limestones were observed at this site.

The outcropping rocks at Turner and Pillinger nunataks are both likely part of the Whichaway Formation (Beacon supergroup) series of sedimentary rocks with cross-cutting sills of Jurassic age Omega dolerite (Ferrar Group) (Brewer, 1989; Elliot & Fleming, 2021; Leat, 2008).

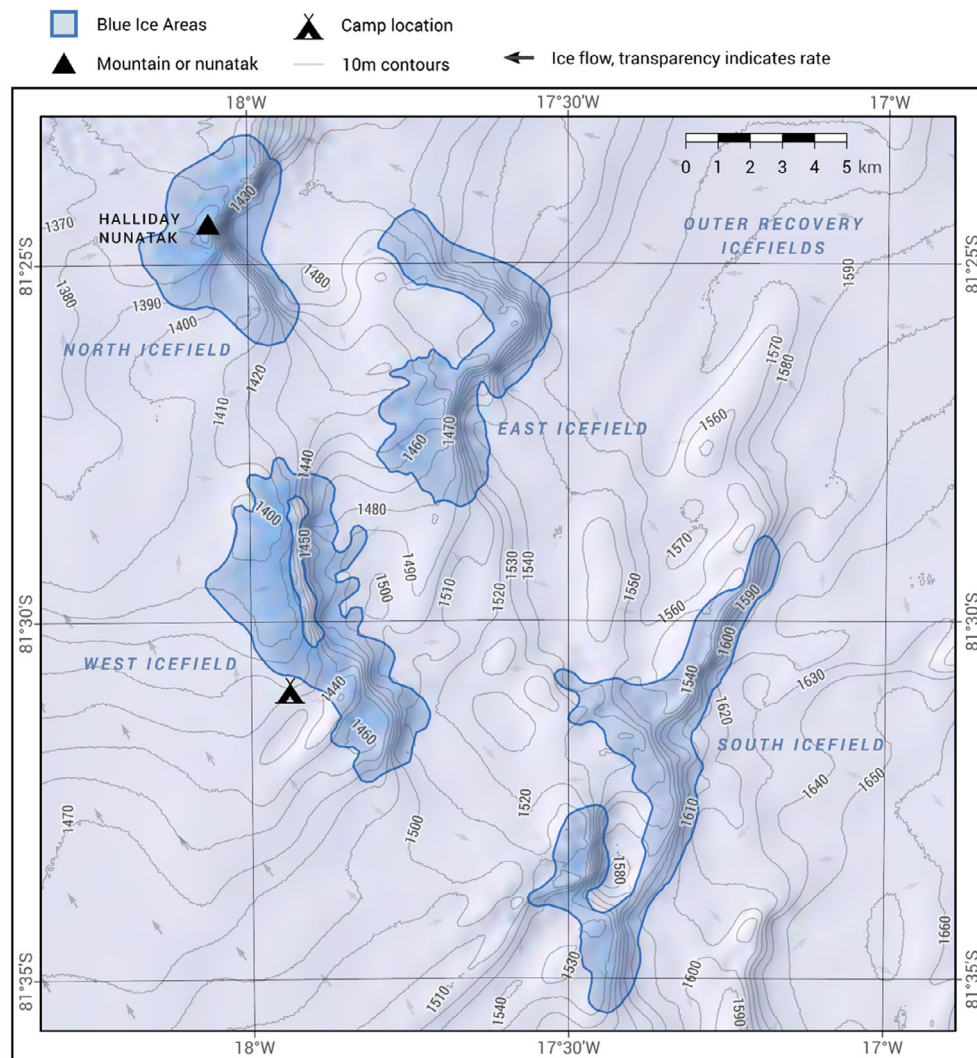


FIGURE 3. The Outer Recovery Icefields dense meteorite collection zone. Meteorites were collected from all the blue icefields in this area: North ($n = 4$), West ($n = 86$), East ($n = 2$), South ($n = 13$) icefields. Camp location shows the position of the 2019–2020 field season main base. 10 m contours are derived from the REMA DEM (Howat et al., 2022). Blue ice areas are taken from Hui et al. (2014). Iceflow velocities from Rignot et al. (2017). Base map is Landsat Image Mosaic of Antarctica (LIMA).

Outer Recovery Icefields Description

The Outer Recovery Icefields comprise four main blue ice areas (Figure 3, Table S2). The icefields are located to the south of the Recovery Glacier, which is sited south of the Shackleton Mountain area of Dronning Maud Land in Norway administered Antarctic territory (Figures 1 and 2). The icefields sit ~ 80 km to the east of the Ramp ice stream (Figure 2). Ice flows into the region from the southwest, from the south part of the Recovery Ice Stream basin catchment (Willis et al., 2016), at velocities between ~ 1 and 16 m year^{-1} (Rignot et al., 2011). The topography of the icefields is relatively flat with slopes typically at $< 5^\circ$. The surface of the blue ice is

variable (Figure 5e,g), ranging from blue and scalloped (rippled), through to cracked and crevassed, and is whiter rippled ice in some places. Areas within individual icefields are sometimes divided by 10–30 m high ice divides that are heavily crevassed. Several debris bands cross the ice surface. The south, west, and east icefields (Figure 3) are all free of surface debris, whereas the north icefield, which is closest to the Outer Recovery Glacier, has some windblown ice surface-bearing rock debris located to the west of Halliday nunatak.

Halliday nunatak, named after astronomer Dr Ian Halliday (1928–2018), is located at $81^\circ 24' 32.97'' \text{S}$, $18^\circ 1' 59.88'' \text{W}$ and is 1554 m high (Figure 3). The outcrop (Figure 8) is composed of quartz-bearing dolerite with

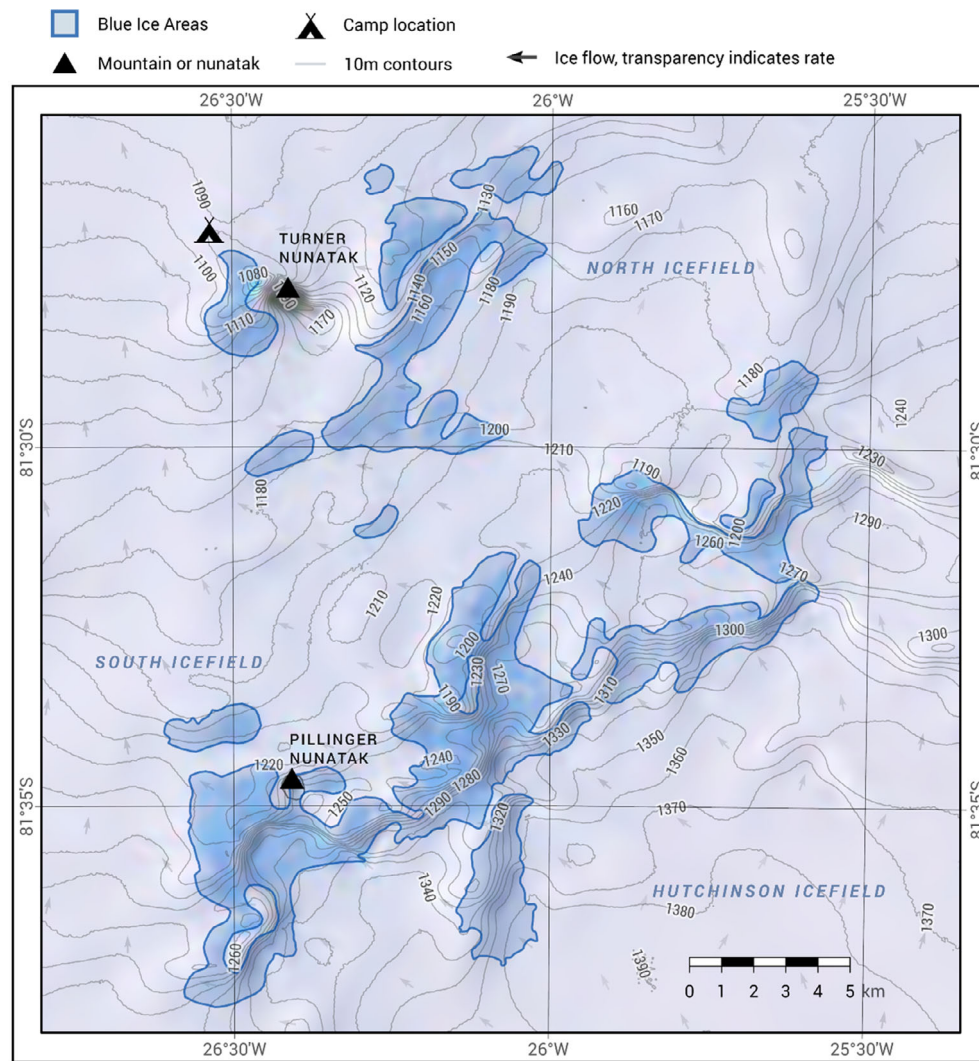


FIGURE 4. The Hutchison Icefield dense meteorite collection zone showing location of Turner Nunatak and five separate blue ice fields that we have divided into a North (two icefields) and a South (three icefields) icefield group. Meteorites were collected from Turner Nunatak ($n = 1$) and from the surrounding blue icefields North ($n = 10$) and South ($n = 5$). Base map is Landsat Image Mosaic of Antarctica (LIMA). 10 m contours are derived from the REMA DEM (Howat et al., 2022). Blue ice areas are taken from Hui et al. (2014). Iceflow velocities from Rignot et al. (2017).

0.5–4 mm crystal size (Figures S4 and S5). Phases present include exsolved pyroxene (1–5 μm lamellae), plagioclase, Ti-oxide, titanomagnetite, with mesostasis regions composed of intergrown quartz and K-feldspar with minor acicular apatite. The sample is coarser grained than the Turner nunatak dyke (see [Hutchison Icefield Description](#) Section), and has higher proportions of K-feldspar and quartz, suggesting it is slightly more chemically evolved. Some regions of the sample have rust staining (Figure S4) and some areas appear to have been weathered to clays. The nunatak surface is heavily weathered dolerite sediment (Figure 8). We carried out U–Pb dating on apatite in sample Z19-3-3a, which returned an intercept date of 164 ± 33 Ma (Figure S6).

This suggests that this outcrop is likely another exposure of the mid-Jurassic aged Ferrar dolerite, which has been observed as sills in the nearby Shackleton Range and Whichaway Nunatak mountains (Elliot & Fleming, 2021; Leat, 2008).

FIELD CAMPAIGN

Hutchison Icefield, with its abbreviated name of HUT was approved as a dense collection area by the Meteoritical Society Nomenclature Committee on January 23, 2021. The Hutchison Icefield region was visited by the project in January 2019 by a two person field party (Katherine Joy and Julie Baum) and revisited

in December 2019 by a different two person field party (Romain Tartèse and Geraint Raymond). Air temperatures in 2019, measured 2 m above the ground, ranged from -2.4 to -13°C . Wind speeds on search days varied from 5 to 20 knots, typically from an easterly prevailing wind direction. The weather during searching was variable, from full sun to near complete cloud cover.

Sixteen meteorites were recovered from the Hutchison Icefield area in the 2018–2019 field season following a reconnaissance search style of searching: that is, random pattern across blue ice on snowmobile driving at speeds of between 5 and 20 km h^{-1} while in an elevated standing position and scanning eyes side to side to identify surface features. Typically, where accessible, one person drove the extent of the edge of the downwind ice seasonal snow line to identify small windblown meteorite samples. Some searching was hindered by recent cover of snowfall, where between 1 and 5 cm of snow was found on, or was observed to fall on, potential blue ice surfaces. One meteorite, Hutchison Icefield 18022, was serendipitously recovered from the surface of Turner nunatak during the 2018–2019 season (Figure 6b).

The Outer Recovery Icefields (OUT) was approved as a dense collection area by the Meteoritical Society Nomenclature Committee on November 2, 2019. The Outer Recovery Icefields region was visited by the Lost Meteorites of Antarctic project in January 2019 by a two person field party (Katherine Joy and Julie Baum), and revisited in December 2019 to January 2020 by a larger field team (Geoffrey Evatt, Rob Taylor, Wouter van Verre, Katherine Joy, Romain Tartèse, Geraint Raymond).

Twenty stones (19 meteorites) were recovered from the Outer Recovery Icefields in the January 2019 field season following mostly reconnaissance search style of searching. In particular, snow cover affected the first (2018–2019) search at Outer Recovery icefields, but a return to the same site in 2019–2020 encountered clearer ice-free surfaces. Eighty-six meteorites were recovered from the area in the December 2019–January 2020 field season following a surface ice systematic search pattern where searches drove in a grid system separated from each other between 5 and 15 m apart.

In total the 2018–2019 two-person team spent 29 days in the field, with 14 days of active surface searching, while the larger 2019–2020 field team spent 40 days in the field, with 19 active surface search days (other days were either camp setup/camp break days, bad weather tent days, or spent deploying the subsurface meteorite detection system—see [Englacial Meteorite Search Efforts](#) Section). In total, 121 meteorites were recovered from the surfaces of the two field sites: 105 meteorites from Outer Recovery, 16 meteorites from Hutchison Icefield.

Englacial Meteorite Search Efforts

The 2019–2020 Outer Recovery Icefields field team deployed an innovative pulse conduction metal detection panel array system (Figure 9), designed to undertake real-time detection and recovery of iron–metal-bearing meteorites (Wilson et al., 2020). The system consisted of a skidoo with an operator control box, dragging a power unit (solar panels and/or battery packs) powering an array of five bespoke pulse induction (PI) metal detectors embedded into polar rated high molecular weight polyethylene (HMWPE) panels (Figure 9). The operator followed real-time handheld GPS tracks (Garmin 64 s) to ensure that they were driving in a grid pattern with overlapping tracks. The dragging effect of the panels also left shallow (<1 cm) groves in the ice surface, which helped guide the operator's track paths. This metal detection panel system was tested in field trials in a temperate climate in the United Kingdom (Peak District, July 2019), in polar conditions in Svalbard (2018 and 2019; Marsh et al., 2020), and in Antarctica at the Sky Blu BAS ice runway (Jan 2019: Figure 9b). These trials determined optimal skidoo speeds, and highlighted numerous technical and signal processing improvements to the system implemented prior to the main field campaign.

The metal detector panels were deployed only at Outer Recovery Icefields west (#OR3) in December 2019 to January 2020 (Figures 3 and 9c). As discussed earlier, this field site was selected on the basis of (1) being the most suitably accessible and flat topography with a large area of non-crevassed ice ideal for driving the skidoo-towed metal detection system, (2) modeling suggested this icefield was likely to be the most meteorite dense zone we could access, and (3) being the most productive meteorite find site in the 2018–2019 reconnaissance field season (15 samples collected from the site). Our estimate of meteorite density used the terrestrial latitudinal meteorite flux of Evatt et al. (2020) to predict that the west icefield had a meteorite number density of 11.34 km^{-2} . Given a realistic “searchable” ice area of 11.25 km^2 (assessed on the 2018–2019 field team's visual inspection of the site and a review of satellite imagery of ice as being crevasse free), the predicted surface number of meteorite finds on this icefield (Outer Recovery west): was in the range 128 ± 33 (where errors represent min and max estimates). Note that this calculation was independent of different meteorite density maps later published by Tollenaar et al. (2022). Using the Evatt et al. (2016) non-iron:iron-rich meteorite Antarctic find ratio we predicted that potentially the missing, englacially trapped, iron meteorites would number 5 for this area (i.e., 0.5 buried meteorite per 1 km^2 of ice). Notably, the total predicted number of meteorites within an MSZ does not take

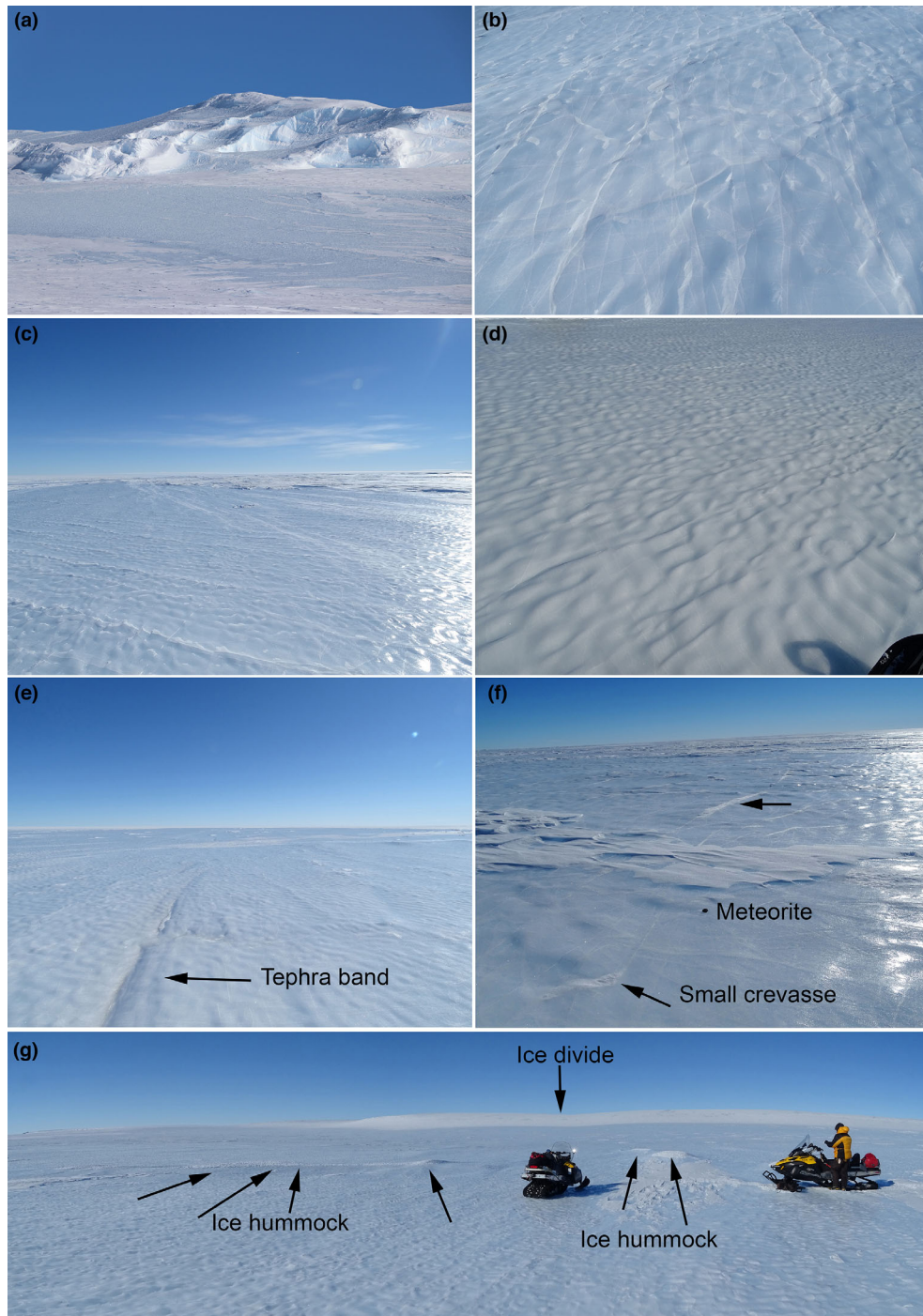


FIGURE 5. Example of ice conditions at (a–d) Hutchison Icefield, and (e–g) Outer Recovery Icefields. (a) 15–20 m high heavily crevassed ice rise (cliff) at Hutchison Icefield located at $\sim 81^{\circ}35'28.30''$ S, $26^{\circ}17'52.10''$ W. (b and c) Typical blue ice surface appearance with small 1–2 cm parallel cracks and suncups (ripples) 2–5 cm in height at Hutchison Icefield. Seasonal snow cover can be seen in (c). (d) Whiter rippled ice at Hutchison Icefield where the ripple height is ~ 2 –3 cm. (e) Example of the surface appearance of an ~ 30 cm wide tephra band in Outer Recovery west icefield. (f) Typical flatter blue ice appearance at Outer Recovery west icefield with small parallel, sometimes sinusoidal crevasses and cracks. Meteorite find OUT 18005 ($3 \times 3 \times 1$ cm) shown for scale. (g) View looking E across the Outer Recovery west icefield looking toward the steep, crevassed, ~ 20 m ice divide. 50 cm to 1 m ice hummocks are indicated in the middle of the view. Skidoos are shown for scale.

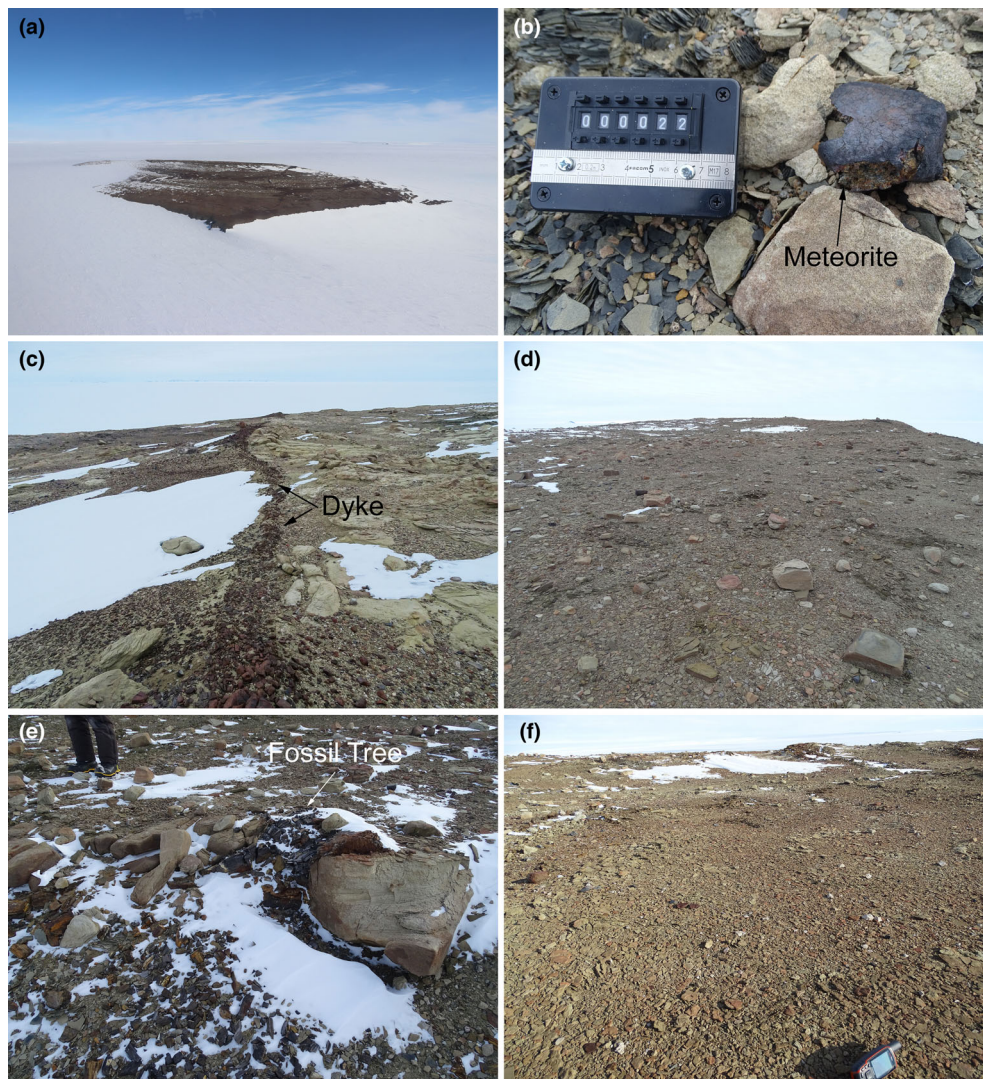


FIGURE 6. Photographs of the surface of Turner Nunatak. (a) Aerial photograph of the nunatak from airplane window—view looking SE. (b) Meteorite sample Hutchison Icefield 18022 recovered from the Turner nunatak surface (field number clicker in photo for scale). (c) At center running top to bottom of image is a basaltic dyke about 1 m in diameter, which is cross-cutting N-S across bedded sandstone units. (d and f) Desert pavement at top of northerly nunatak, formed from interlocking siltstones with larger sandstone dropstones. (e) Bedded sandstone unit (about 1 m thick) with large embedded petrified wood tree (dark colored rocks at center). Photos: Katherine Joy/The University of Manchester.

account of the fraction of localized or transient snow cover an MSZ might experience during a particular field season (e.g., if it is 50% covered in snow, then the corresponding expected number of recoverable meteorites should be halved). From a crude visual inspection, the snow cover during the 2019–2020 season appeared to be around 30%, meaning the predicted number of recoverable meteorites from Outer Recovery west was 30% less than 128 ± 33 , that is, 90 ± 23 , which is consistent with the number recovered from this icefield: 105.

A test campaign was initiated at the field site to (i) test the equipment drivability, and (ii) test each individual

panel and control box to optimize the electronic signal processing. The latter employed a $\sim 2.5 \times 2.5$ cm, 100 g, analog iron meteorite (a small iron cylinder) buried at different depths in the ice down to ~ 50 cm. These tests suggested that given the rough ice sculptured surface 10 km h^{-1} was the most suitable safe driving conditions and the metal detection signal processing was adapted to this speed. The system was then deployed with the operator dragging the panels in a systematic search grid watching for real-time alerts for metal-rich objects. Some surface meteorites were found during these searches, where the panel system was stopped at least 5 m from the

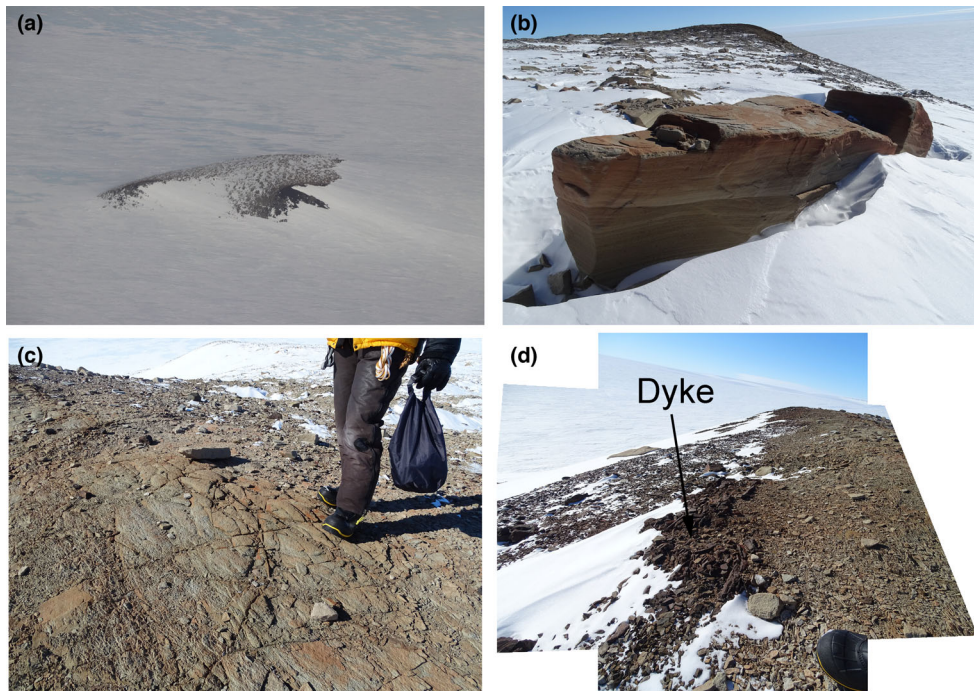


FIGURE 7. (a) Aerial view (from plane window) of Pillinger nunatak looking SW. (b) View of the nunatak looking W with a large-bedded sandstone boulder. Nunatak surface (c) sandstone fractured surface, and (d) a basaltic dyke (left) contacting against sandstone (right of photo). Photos: Katherine Joy/The University of Manchester.

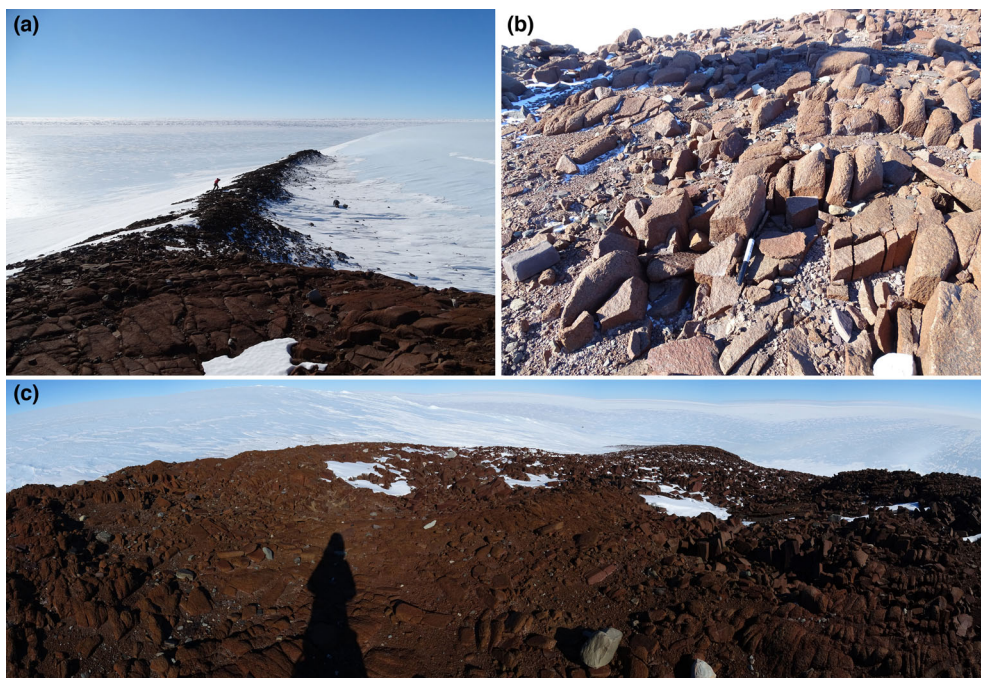


FIGURE 8. Photos of Halliday nunatak in the northern most Outer Recovery Icefields. (a) View from the nunatak peak looking north toward the Recovery Glacier, note two people in frame for scale. (b) and (c) Surface of nunatak showing heavily weathered gabbro surface, where image (c) is a panorama. Photos: Katherine Joy/The University of Manchester.

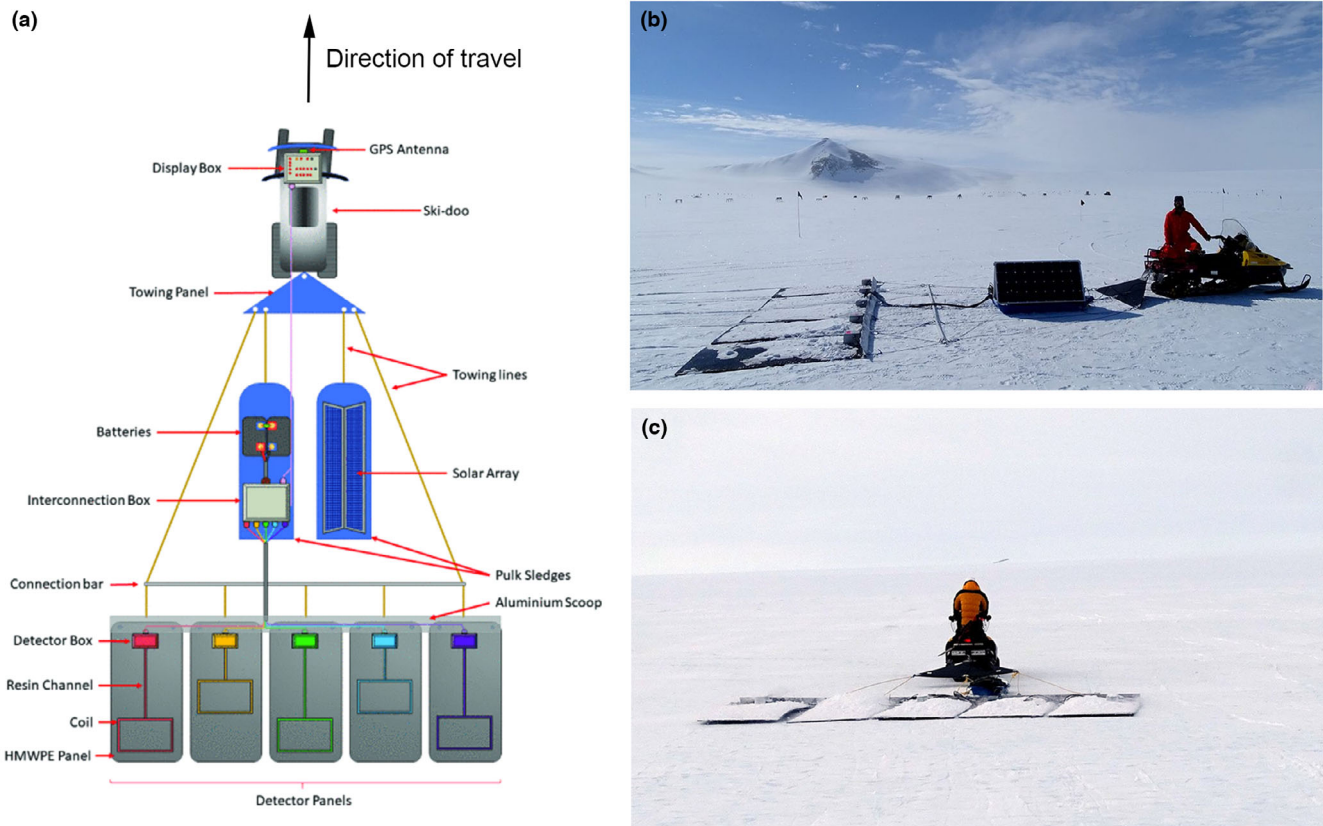


FIGURE 9. Lost Meteorites of Antarctica project subsurface meteorite detection system. (a) Birds eye view schematic of full metal detector panel system (modified from Marsh et al., 2020). (b) Full detection system deployed at Sky Blu in January 2019 (Photo: Mike Rose/BAS). (c) Full detection system deployed at Outer Recovery Icefields in December 2019. At this stage of the field campaign, the solar panel unit had failed and so there is only one sledge deployed between the skidoo and the metal detection panels, and the system was running off battery power. Photo: Katherine Joy/The University of Manchester. Note in (c) that 1–2 cm of overnight snow had fallen, meaning that we could not spot any surface meteorites during the search as they were snow-covered, although the snow was very useful for clearly denoting where the panel system had been dragged across the (now snow covered) blue ice field.

surface-spotted sample to minimize demagnetization (Vervelidou, Weiss, & Lagroix, 2023). Data logged by each coil system were reviewed each night after the panel deployment to postprocess to see if any signals in the field had been missed in real time. The team encountered many false-positive signals from the system, when an alert would sound/visual display would light up, but upon driving over the same area repeated times the signal trigger was not replicated. Many areas were tested using a Vallon hand-held metal detector to double check that there were no metal-rich objects present. Successful metal-rich detections included at least one metal screw, which had fallen off the equipment, and a spanner that had been accidentally dropped on the ice surface and buried by overnight snowfall. The combination of harsh environmental conditions and extended hours of use meant that various components of the equipment broke and had to be replaced/fixed or were declared

non-salvageable. These included: the electronic components within coil detector logging and signal processing systems; the metal hardware itself (bolts, connections) on the panel rig; the solar panels power system, an automotive rated 12 V lead acid battery, and the base of one of the power unit sledges. Analysis of the physical damage, and the measurements taken by accelerometers mounted in the metal detector boxes, demonstrated that the vibration encountered (Figure 11) of the direct contact between the panels and scalloped (suncupped) ice with adhering seasonal snow patches (Figure 5b–f) at the Outer Recovery west icefield was much higher than anticipated from the relatively smoother ice/snow-covered ice test sites in the Arctic Svalbard and Sky Blu Antarctic (Figure 9c) field trials. We also observed that there was more movement between the individual panels in the field than we expected from the field trials. This was also caused by the more uneven



FIGURE 10. Examples of meteorites recovered during the Lost Meteorites of Antarctica field campaigns. (a) Sample HUT 18036 (photo labeled with number 000036)—ordinary chondrite (H6) found partially enclosed in ice. (b) Sample OUT 19109 (photo labeled with number 000109)—ordinary chondrite (H6) found partially enclosed in ice. (c) Sample OUT 18011 (photo labeled with number 000011)—ordinary chondrite (H6) with a fresh black fusion crust (95% coating) on ice surface. (d) Sample OUT 18012 a carbonaceous chondrite (CM-an) (photo labeled with number 000011). (e) Sample HUT 18021—ordinary chondrite (L6) (photo labeled with number 000021) and (f) Sample OUT 18014 a mesosiderite (photo labeled with number 000013).

terrain (i.e., sculptured ice surface), which caused each panel to move faster in respect to the surrounding panels causing more electronic interference between the systems than we expected.

After 18 days of running the metal detector searches when a total of ~ 0.74 km² of the ice had been searched, a decision was taken by the team in the field and wider team back in the United Kingdom that the equipment was no longer useable as a reliable system, and the

subsurface meteorite search part of the expedition was terminated (Amos, 2020). Regrettably, with only ~ 0.74 km² of metal detection panel coverage, the experiment did not cover enough ice to test the 0.5 iron-rich buried meteorites per square km of ice hypothesis (Evatt et al., 2016). However, additional time spent in the field at the end of the experiment meant that the field team were able to complete the ice surface searching activities of the Outer Recover Icefields.

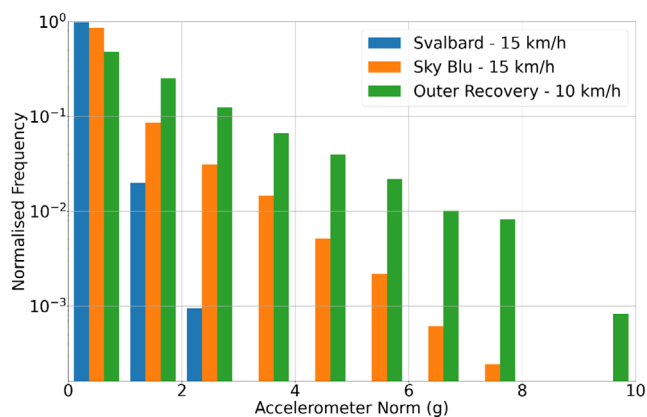


FIGURE 11. Normalized histogram of representative accelerometer measurements from the meteorite detection system. Each data set consists of six repetitions of linear scans taken in Svalbard in March 2019 (78.92424 N, 11.88313 E), Sky Blu in December 2018 (74.85716 S, 70.56016 W), and Outer Recovery west icefield in December 2019 (81.50526 S, 17.94064 W). Note that saturation of the accelerometer data occurs at 10 g. The data clearly show that even at lower velocities of operation (i.e., 10 km h⁻¹) at Outer Recovery west the metal detection system routinely witnessed much higher vibrations (i.e., >3.5 g, peaks between 6 and 10 g) relative to the Svalbard (max 2.5 g) and Sky Blu (max 7 g) test sites.

SCIENCE OUTCOMES AND FUTURE PROSPECTS

In total, 121 meteorites were collected from surface ice at Hutchison Icefield and Outer Recovery Icefields in two austral summer field seasons in 2018–2019 and 2019–2020: Examples are shown in Figure 10. The theoretical work regarding the prediction of fruitful new MSZs published by Evatt et al. (2020) will be of use to future recovery missions hoping to prioritize new blue ice areas to visit, especially given its evident success in relation to the returned meteorites through this project. In addition to the scientific efforts, the project also ran a popular online blog post documenting in-field efforts and project progress (via www.antarcticmeteorites.wordpress.com) and was covered by national and international news outlets.

The recovered meteorites were returned to the United Kingdom for scientific study. The meteorites (Figure 10) were returned as frozen cargo from the field, via the BAS Halley and Rothera research stations, and then as frozen stow on a BAS research ship. The frozen samples were received for preliminary examination and curation at the University of Manchester, United Kingdom (MacArthur, Joy, Harvey, Jones, Evatt, Almeida, Malley, Greenwood, Findlay, & King, 2022) and are in the process of being classified (Gattacceca et al., 2022, 2023; MacArthur, Joy, Harvey, Jones, Evatt, Almeida, Malley, Greenwood, & Findlay, 2022; Meteoritical Bulletin, 2023). The sample curation and initial analysis are discussed in Joy et al. (2021), MacArthur, Joy, Harvey, Jones, Evatt,

Almeida, Malley, Greenwood, Findlay, and King (2022) and MacArthur, Joy, Harvey, Jones, Evatt, Almeida, Malley, Greenwood, & Findlay (2022) and Harvey et al. (2023). A summary of the meteorite types and statistics will be discussed in depth in future papers. The type specimen and main mass meteorites recovered by the project have been transferred to the Natural History Museum (NHM), London, and are available upon request for scientific analysis by contacting the NHM Meteorite Curator.

The Lost Meteorites of Antarctica project developed and deployed a novel metal detection system, designed to locate englacially trapped iron-rich meteorites (Marsh et al., 2020). Our project demonstrates the extreme challenges of Antarctic fieldwork: despite rigorous testing of the equipment, and a team experienced in deploying electronic equipment and hardware to remote fieldwork locations and polar settings, and our team's best efforts, the equipment in the field did not ultimately cover enough of the ice field we searched to test the Evatt et al. (2016) "Missing Iron Meteorite" hypothesis. We hope that future meteorite recovery programs are able to solve the mystery of Antarctic meteorite type collection statistics (Corrigan et al., 2014) before meteorites are further lost from the ice surface by climate change-induced global heating (Tollenaar et al., *in press*).

Acknowledgments—The Lost Meteorites of Antarctica project was supported by the Leverhulme Trust (grant RPG-2016-349), The BAS/NERC, and University of Manchester internal Faculty of Science and Engineering funding. Funding is also acknowledged from the Royal Society (KJ: URF\R\201009; KJ, JM: RF\ERE\210158) and STFC (KJ, RJ, RT: ST/V000675/1, a PhD studentship to TH). We also thank the University of Manchester and STFC (grant ST/S002170/1) for funding the LA-ICP-MS facility. IDA received funding from EPSRC (grant EP/R014604/1 and EP/K032208/1). Antarctic fieldwork is hard: huge thanks to all the wonderful BAS pilots, field logistics teams, science support, and research station staff for all their incredible efforts to get our field team out and back from the field sites, to feed us and look after us so well. The field party thank the team back in the United Kingdom who helped troubleshoot the equipment issues and help run the public engagement blog remotely. Drs John Cowpe and Lydia Fawcett are thanked for their support of the Isotope Group laboratory facilities used to receive the samples in Manchester. The NHM Meteorite Curator Dr Natasha Almeida is thanked for her efforts in the long-term curation of the samples. We thank the two reviewers of this manuscript and editor Marc Caffee for their constructive feedback and suggestions.

Editorial Handling—Dr. Marc W. Caffee

REFERENCES

- Amos, J. 2020. UK Meteorite Hunt Thwarted by Equipment Damage. <https://www.bbc.co.uk/news/science-environment-51040336>.
- Annexstad, J. O. 1986. Meteorite Concentration Mechanisms in Antarctica. In Lunar and Planetary Inst, International Workshop on Antarctic Meteorites.
- Bintanja, R. 1999. On the Glaciological, Meteorological, and Climatological Significance of Antarctic Blue Ice Areas. *Reviews of Geophysics* 37: 337–359.
- Brewer, T. S. 1989. Mesozoic Dolerites from Whichaway Nunataks. *Antarctic Science* 1: 151–55.
- Cassidy, W., Harvey, R., Schutt, J., Delisle, G., and Yanai, K. 1992. The Meteorite Collection Sites of Antarctica. *Meteoritics* 27: 490–525.
- Cassidy, W. A. 2012. *Meteorites, Ice, and Antarctica: A Personal Account*. Cambridge University Press.
- Cassidy, W. A., Schutt, J., Koeberl, C., Yanai, K., Lindner, L., and Mardon, A. 1987. The Meteorite Concentration at the Lewis Cliff, Antarctica, Ice Tongue. *Meteoritics* 22: 353.
- Choi, B. G., Ahn, I., Lee, J. I., and Park, C. 2009. Classification and Petrological and Geochemical Characteristics of Antarctic Meteorites Found by 1st, 2nd and 3rd KOREAMET.
- Corrigan, C. 2011. Antarctica: The Best Place on Earth to Collect Meteorites. *Elements* 7: 296.
- Corrigan, C. M., Welzenbach, L. C., Righter, K., McBride, K. M., McCoy, T. J., Harvey, R. P., and Satterwhite, C. E. 2014. A Statistical Look at the US Antarctic Meteorite Collection. In *In 35 Seasons of US Antarctic Meteorites (1976–2010): A Pictorial Guide to the Collection*, 173–187. Washington, DC/Hoboken, NJ: American Geophysical Union/John Wiley & Sons, Inc.
- Corti, G., Zeoli, A., and Bonini, M. 2003. Ice-Flow Dynamics and Meteorite Collection in Antarctica. *Earth and Planetary Science Letters* 215: 371–78.
- Debaille, V., Goderis, S., Kaiden, H., and Claeys, P. 2011. Search for Antarctic Meteorites, Belgian Approach. *Newsletter of Geologica Belgica*: 7–7.
- Delisle, G., Franchi, I., Rossi, A., and Wieler, R. 1993. Meteorite Finds by EUROMET Near Frontier Mountain, North Victoria Land, Antarctica. *Meteoritics* 28: 126–29.
- Elliot, D. H., and Fleming, T. H. 2021. Chapter 2.1b Ferrar Large Igneous Province: Petrology. *Geological Society, London, Memoirs* 55: 93–119. <https://doi.org/10.1144/M55-2018-39>.
- Evatt, G. W., Coughlan, M. J., Joy, K. H., Smedley, A. R. D., Connolly, P. J., and Abrahams, I. D. 2016. A Potential Hidden Layer of Meteorites below the Ice Surface of Antarctica. *Nature Communications* 7: 10679.
- Evatt, G. W., Smedley, A. R. D., Joy, K. H., Hunter, L., Tey, W. H., Abrahams, I. D., and Gerrish, L. 2020. The Spatial Flux of earth's Meteorite Falls Found Via Antarctic Data. *Geology* 48: 683–87.
- Faure, G. 1990. Supraglacial Moraines, Associated Meteorites and Climate Change. In *Antarctic Meteorite Stranding Surfaces*, 34. Houston, TX: Lunar and Planetary Institute.
- Folco, L., Capra, A., Chiappini, M., Frezzotti, M., Mellini, M., and Tabacco, I. E. 2002. The Frontier Mountain Meteorite Trap (Antarctica). *Meteoritics & Planetary Science* 37: 209–228.
- Fretwell, P., Pritchard, H. D., Vaughan, D. G., Bamber, J. L., Barrand, N. E., Bell, R., Bianchi, C., et al. 2013. Bedmap2: Improved Ice Bed, Surface and Thickness Datasets for Antarctica. *The Cryosphere* 7: 375–393.
- Gattacceca, J., McCubbin, F. M., Grossman, J., Bouvier, A., Chabot, N. L., d'Orazio, M., Goodrich, C., et al. 2022. The Meteoritical Bulletin, No. 110. *Meteoritics & Planetary Science* 57: 2102–5. <https://doi.org/10.1111/maps.13918>.
- Gattacceca, J., McCubbin, F. M., Grossman, J. N., Schrader, D. L., Chabot, N. L., D'Orazio, M., Goodrich, C., et al. 2023. The Meteoritical Bulletin, No. 111. *Meteoritics & Planetary Science*. <https://doi.org/10.1111/maps.13995>.
- Harvey, R. 2003. The Origin and Significance of Antarctic Meteorites. *Geochemistry* 63: 93–147.
- Harvey, R. P., Schutt, J., and Karner, J. 2014. Fieldwork Methods of the US Antarctic Search for Meteorites Program. In *35 Seasons of US Antarctic Meteorites (1976–2010): A Pictorial Guide to the Collection*, 23–41. Washington, D.C; Hoboken, New Jersey: American Geophysical Union; John Wiley & Sons, Inc.
- Harvey, T. A., MacArthur, J. L., Joy, K. H., Sykes, D., Almeida, N. V., and Jones, R. H. 2023. Nondestructive Determination of the Physical Properties of Antarctic Meteorites: Importance for the Meteorite—Parent Body Connection. *Meteoritics & Planetary Science*. 58: 1707–46. <https://doi.org/10.1111/maps.14094>.
- Howat, I., Porter, C., Noh, M. J., Husby, E., Khuvis, S., Danish, E., Tomko, K., et al. 2022. The Reference Elevation Model of Antarctica—Strips, Version 4.1, Harvard Dataverse, V1 <https://doi.org/10.7910/DVN/EBW8UC>.
- Hui, F., Ci, T., Cheng, X., Scambo, T. A., Liu, Y., Zhang, Y., Chi, Z., et al. 2014. Mapping Blue-Ice Areas in Antarctica Using ETM+ and MODIS Data. *Annals of Glaciology* 55: 129–137.
- Imae, N., Akada, Y., Berclaz, C., Claeys, P., Debaille, V., Goderis, S., Hublet, G., et al. 2013. The Search for Antarctic Meteorites in the Nansen Ice Field by the Joint Team of Japan and Belgium. Proceedings of Japan Geoscience Union Meeting.
- Joy, K. H., MacArthur, J. L., Harvey, T. A., and Jones, R. H. 2021. The Lost Meteorites of Antarctica: Field Campaigns and Coordinated Sample Analysis Approach to Preliminary Scientific Study. Goldschmidt 2021 Virtual 4–9 July, ORAL-AM-75.
- Kojima, H. 2006. The History of Japanese Antarctic Meteorites. *Geological Society, London, Special Publications* 256: 291–303.
- Leat, P. T. 2008. On the Long-Distance Transport of Ferrar Magmas. *Geological Society, London, Special Publications* 302: 45–61.
- MacArthur, J. L., Joy, K. H., Harvey, T. A., Jones, R. H., Evatt, G. W., Almeida, N. V., Malley, J., Greenwood, R. C., and Findlay, R. 2022. Four New Antarctic Achondrites Recovered by the Lost Meteorites of Antarctica Project. *LPI Contributions* 2678: 1996.
- MacArthur, J. L., Joy, K. H., Harvey, T. A., Jones, R. H., Evatt, G. W., Almeida, N. V., Malley, J., Greenwood, R. C., Findlay, R., and King, A. J. 2022. Lost Meteorites of Antarctica Project: Classifications to Date. *Meteoritics & Planetary Science* 57: 6414.
- Marsh, L. A., Van Verre, W., Wilson, J., Evatt, G. W., and Peyton, A. J. 2020. Evaluation of a Bespoke Antarctic Meteorite Detection System in Polar Operating Conditions. In *2020 IEEE Sensors Applications Symposium (SAS)*, 1–5. IEEE.
- Marvin, U. B. 2014. The Origin and Early History of the US Antarctic Search for Meteorites Program (ANSMET). In

- In 35 Seasons of US Antarctic Meteorites (1976–2010): A Pictorial Guide to the Collection*, 1–22. Washington, D.C.; Hoboken, NJ: American Geophysical Union; John Wiley & Sons, Inc.
- Metoritical Bulletin 2023. Accessed July 2023. <https://www.lpi.usra.edu/meteor/>
- Nagata, T. 1978. A Possible Mechanism of Concentration of Meteorites within the Meteorite Ice Field in Antarctica. *Memoirs of National Institute of Polar Research. Special issue* 8: 70–92.
- Park, C., Baek, J., Ha, S., Nagao, K., Park, S., Ahn, I., Moon, J. J., Yoo, I. S., and Lee, J. I. 2015. Report on Classification of Antarctic Meteorites from the 2014/15 KOREAMET Season. 2015.10.28~2015.10.30 <https://repository.kopri.re.kr/handle/201206/7137>.
- Righter, K., Corrigan, C., McCoy, T., and Harvey, R. 2014. *35 Seasons of US Antarctic Meteorites (1976–2010): A Pictorial Guide to the Collection*. Washington, D.C.; Hoboken, New Jersey, American Geophysical Union; John Wiley & Sons, Inc.
- Rignot, E., Mouginot, J., and Scheuchl, B. 2011. *MEaSURES InSAR-Based Antarctica Ice Velocity Map, Version 1* [Indicate subset used]. Boulder, CO: NASA National Snow and Ice Data Center Distributed Active Archive Center. <https://doi.org/10.5067/MEASURES/CRYOSPHERE/nsidc0484.001>.
- Rignot, E., Mouginot, J., and Scheuchl, B. 2017. *MEaSURES InSAR-Based Antarctica Ice Velocity Map, Version 2*. Boulder, CO: NASA National Snow and Ice Data Center Distributed Active Archive Center. <https://doi.org/10.5067/D7GK8F5J8M8R>.
- Smedley, A. R., Evatt, G. W., Mallinson, A., and Harvey, E. 2020. Solar Radiative Transfer in Antarctic Blue Ice: Spectral Considerations, Subsurface Enhancement, Inclusions, and Meteorites. *The Cryosphere* 14: 789–809.
- Tollenaar, V., Zekollari, H., Lhermitte, S., Tax, D. M., Debaille, V., Goderis, S., Claeys, P., and Pattyn, F. 2022. Unexplored Antarctic Meteorite Collection Sites Revealed through Machine Learning. *Science Advances* 8: eabj8138.
- Tollenaar, V., Zekollari, K. C., Farinotti, D., Lhermitte, S., Debaille, V., Goderis, S., Claeys, P. J. K. H., and Pattyn, F. Accepted In Press. Antarctic Meteorite Archives Threatened by Ongoing and Future Climate Warming. *Nature Climate Change*.
- Vervelidou, F., Weiss, B. P., and Lagroix, F. 2023. Hand Magnets and the Destruction of Ancient Meteorite Magnetism. *JGR-Planets* 128: e2022JE007464. <https://doi.org/10.1029/2022JE007464>.
- Wadhwa, M., McCoy, T. J., and Schrader, D. L. 2020. Advances in Cosmochemistry Enabled by Antarctic Meteorites. *Annual Review of Earth and Planetary Sciences* 48: 233–258.
- Whillans, I. M., and Cassidy, W. A. 1983. Catch a Falling Star: Meteorites and Old Ice. *Science* 222: 55–57.
- Willis, I. C., Pope, E. L., Gwendolyn, J. M., Arnold, N. S., and Long, S. 2016. Drainage Networks, Lakes and Water Fluxes beneath the Antarctic Ice Sheet. *Annals of Glaciology* 57: 96–108.
- Wilson, J. W., Marsh, L. A., Van Verre, W., Rose, M. C., Evatt, G. W., Smedley, A. R. D., and Peyton, A. J. 2020. Design and Construction of a Bespoke System for the Detection of Buried, Iron-Rich Meteorites in Antarctica. *Antarctic Science* 32: 58–69.
- Yoshida, M., Hisao, A. N. D. O., Omoto, K., Naruse, R., and Ageta, Y. 1971. Discovery of Meteorites near Yamato Mountains, East Antarctica. *Antarctic Materials* 39: 62–65. [doi/10.15094/00007603](https://doi.org/10.15094/00007603).
- Zhang, M., and Haward, M. 2022. The Chinese Antarctic Science Programme: Origins and Development. *Antarctic Science* 34: 191–204.
- Zhou, C., Ai, S., Chen, N., Wang, Z., and Dongchen, E. 2011. Grove Mountains Meteorite Recovery and Relevant Data Distribution Service. *Computers & Geosciences* 37: 1727–34.

SUPPORTING INFORMATION

Additional supporting information may be found in the online version of this article.

Data S1. Methods for analysis of terrestrial rock samples.

Table S1. Summary of the Hutchison Icefield localities. The numbers in parentheses in the first column represent the field number scheme used in some of our field notes. The BAS ID number relates to the British Antarctic Survey sample number of the rock / mineral debris collected at the location.

Table S2. Summary of the Outer Recovery Icefields localities. The numbers in parentheses in the 1st column

represent the field number scheme used in some of our field notes. The BAS ID number relates to the British Antarctic Survey sample number of the rock / mineral debris collected at the location.

Table S3. Protocols for analysis of sample dates and trace elements using laser ablation inductively coupled mass spectrometry (LA-ICP-MS) at the University of Manchester.

Table S4. U-Pb dates of apatite in sample Halliday nunatak dolerite sample Z19-3-3a and in standards.

Table S5. Trace element concentrations of apatite in sample Halliday nunatak dolerite sample Z19-3-3a and in standards.